Proceedings of the Forty-first Turbomachinery Symposium
September 24-27, 2012, Houston, Texas

Evaluation of Bearing Designs for a Multistage Centrifugal Compressor Using a Magnetic Exciter

Donghui Zhang
Manager, Gas Compressor Overhaul and Restage Engineering
Solar Turbines, Inc
San Diego, CA, USA

Wolfgang Faller
Manager, Gas Compressor Mechanical Design
Solar Turbines, Inc
San Diego, CA, USA

Chester Lee
Manager, Gas Compressor Rotordynamics
Solar Turbines, Inc
San Diego, CA, USA

Donghui Zhang is the manager of the Gas Compressor Overhaul and Restage Engineering Group at Solar Turbines Inc. in San Diego, CA. Dr. Zhang joined Solar in 2004 after graduating from Michigan State University with a Ph.D. degree in Mechanical Engineering. He has experience in areas of aerodynamics and rotordynamics of gas compressor design.

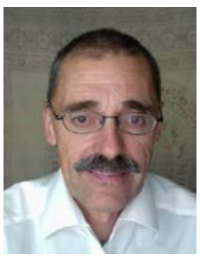

Wolfgang Faller is the manager of mechanical design at Solar Turbines' Gas Compressor Business, overseeing advanced technology introduction, new product development as well as engineering maintenance the existing natural gas compressor product line. Prior to joining Solar in San Diego, he held positions at Concepts NREC, Woburn MA, Linnig Trucktec, Markdorf and Sulzer in Ravensburg, Germany. Over his career he was involved in ship propellers, hydraulic turbines, steam turbines, integral gear compressors, expanders, heavy duty truck components, turbochargers and natural gas compressors. Dr. Faller holds an MBA from Norwich University, a doctorate and an engineering diploma in Naval Architecture from Technische Universität Berlin, Germany.

Chester C. Lee is the Manager of Rotordynamics Design and Test in the Gas Compressor Engineering Department of Solar Turbines Inc., in San Diego, California. His major responsibility is to support rotordynamic analysis in design, manufacturing, testing, and field operation. Dr. Lee received his Ph.D. degree majoring in Mechanical Engineering from the University of Virginia, specializingin rotating machinery. Before joining Solar, he worked for Mechanical Technology Inc., in Latham, New York, on various rotating equipment.

ABSTRACT

The amount of damping in the rotor/bearing system is the key to stability of centrifugal gas compressors, especially for rotors with high slenderness ratio. A full pressure performance test can certainly demonstrate whether a rotor is stable or not. But the drawback is that it cannot quantify the amount of damping in the system prior to the instability threshold. Alternatively, the rotor can be subjected to disturbances by applying a force acting on the rotor and the response from the rotor allows us to measure the amount of damping through vibration amplitude changes.

In this paper, we will discuss a magnetic exciter system that was designed to inject a known force at one end of the rotor while the rotor is operating at different loaded conditions. The compressor rotor was excited by magnetic forces and its response was observed for evaluating the damping of the system. Different techniques were used to estimate rotor stability and were evaluated in this study.

This test arrangement can also be used to evaluate different journal bearing designs. Data from a centrifugal compressor test using three different tilting pad bearings are compared and discussed. The test data shows that for the compressor investigated, the 5-pad tilting pad bearing design is better than the two 4-pad bearings.

The stability threshold as a function of discharge pressure is also presented in this paper. A good agreement between prediction and test data was achieved when taking into account certain aerodynamic excitation mechanisms.

The system provides a technically sound and economic enhancement to the design process: validation of full-pressure stability margin, back-to-back comparison of components such as bearings as well as valuable insight into rotor – and aerodynamic interactions.

INTRODUCTION

Ever more challenging environments in the Oil and Gas industry push compressor designers to incorporate more compression duties into pressure vessels with increased rating. To achieve a high-pressure ratio, the compressor needs a long bearing span to allow more compression stages. At the same time, the trend to increase power-density leads to faster running compressors with high flow coefficients for high power applications, which means that the compressor is pumping large volumes of high-density fluids. The longer bearing span reduces the critical speed and the dense fluids increase the seal cross coupling forces significantly. Many applications push the rotor into lower critical speed ratio and high-density regions that will require level II analysis per API 617 (2002).

End users usually require full power, full speed compressor testing at the factory due to uncertain predictions of the cross coupling forces in the seals. To obtain more information about rotor stability during full power testing, a magnetic exciter can be attached to one end of the rotor to inject a force to the rotor/bearing system. The rotor response can be measured and the system stability (δ or Log Dec) can be quantified.

Rotor Stability Identification

There are different ways to conduct magnetic exciter tests, one of them, the frequency response function (FRF) method, is very popular in the industry. An external force from an actuator is applied to the rotor, typically at the non-driven end. The force sweep in the frequency domain leads to a rotor response that is observed. To estimate δ, the rotor can be treated as either a single degree of freedom (SDOF) or multi degree of freedom (MDOF) system.

When the rotor is treated as a single degree of freedom system, δ can be easily calculated through Equations (1) and (2).

$$\delta = \frac{2\pi\zeta}{\sqrt{1-\zeta^2}} \qquad (1)$$

$$\zeta = \frac{1}{2AF} \qquad (2)$$

To estimate the system damping ratio ζ, the amplification factor (AF) is obtained from the Bode plot with a forward circular excitation sweeping through the 1st critical natural frequency. Among others, Atkins and Perez (1990) implemented this method by injecting the force to the bearing pedestal via a shaker.

As magnetic bearing technology was developed quickly in the 1990's, using a magnetic bearing to excite the rotor became a new way to perform non-synchronous excitation testing. Baumann (1999) reported magnetic bearing exciter testing on a high-pressure compressor. Then Moore, et al (2002) and Moore and Soulas (2003) published more stability data on industry compressors using a magnetic exciter, followed by more papers using a similar method (Gupta, et al,2008), Soulas and Kuzdal (2009), Sorokes, et al (2009)). Bidaut, et al(2009) did the calculation slightly different, they obtained the damping ratio directly by curve-fitting the Nyquist plot. In their paper, it was mentioned that the forward and backward excitation mainly excites the corresponding mode. This is an important observation proposing to estimate the system stability by forward excitation FRF.

A Bode plot from a typical forward circular excitation response is shown in Figure 1. The signals with dashed lines are the overall vibration data, the signals with solid lines are the vibration level at the excitation frequency (synchronous to excitation frequency). The amplification factor is calculated by using the response that is synchronous to excitation frequency. In this particular case, the vibration level at the suction end (exciter end) did not change much after passing the 1st critical frequency, so the amplification factor is calculated based on the discharge end (non exciter end) responses.

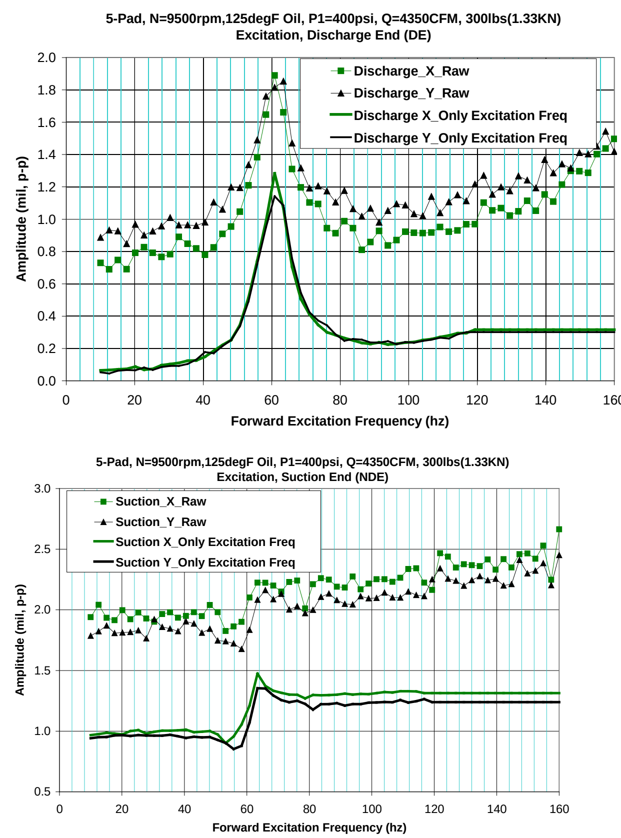

Figure 1. A Typical Bode Plot from Forward Circular Excitation Response

Once ζ is calculated via the amplification factor from the Bode plot, δ can be easily obtained from equation (1).

The other method to determine δ is to measure the transient response in the time domain after the excitation force has been removed. δ can also be defined as the rate of change for an oscillatory signal:

$$\delta = \frac{1}{n}\ln\left(\frac{X_0}{X_n}\right) = \frac{2\pi\alpha}{\omega} \quad (3)$$

where

X_0 is the initial displacement

X_n represents the amplitude after n cycles have elapsed.

For a given decaying signal it can be expressed by

$$X = X_0 e^{(-\alpha + i\omega)t} \quad (4)$$

where

X_0 is the initial condition,

α is the growth factor, and

ω is the frequency

Two slightly different methods can be used to determine δ in the time domain:

- By directly applying the amplitude ratio in equation (3)
- By the decay rate of the signal vibration envelope, $X = X_0 e^{-\alpha t}$

This method is different from FRF. Instead of obtaining the rotor response in the frequency domain, the rotor response in the time domain is observed. The transient signals are processed and δ is calculated. The rotor is treated as a single degree of freedom (SDOF) system.

Figure 2 shows a typical transient response when a steady forward circular excitation was shut down after about 0.2 seconds of excitation. The upper plot shows the raw signals and the lower plot depicts signals that were processed with a 5th order low-pass filter with a cutoff frequency of 10 Hz above the 1st critical natural frequency.

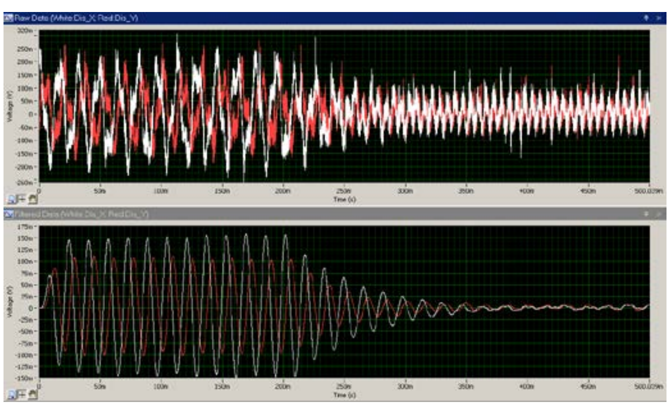

Figure 2. Forward Excitation Transient Signal (400lbf at 62hz, 9500rpm, 5-pad Brg, 145degF Oil, 50psi Inlet Pressure): Transient Time Domain Response

The spectrum of raw signals before the excitation forces were shut down is plotted in Figure 3. It shows only two dominant signal components: at the excitation frequency (coinciding with the 1st natural frequency) and the compressor running speed. The spectrum is very clean without noise at lower frequencies.

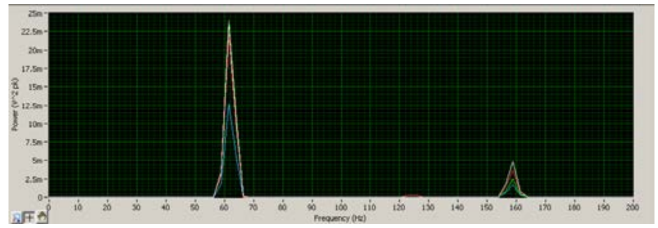

Figure 3. Spectrum During Steady State

The filtered signal decay envelopes for both axes of vibration were best-fitted as shown in Figure 4. δ was then calculated using Equation (3).

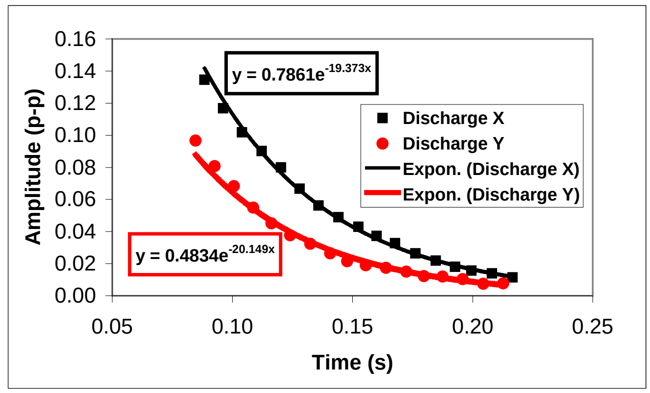

Figure 4. The Signal Decay in Transient Forward Circular Excitation

Compared to SDOF methods, multiple degree of freedom (MDOF) methods are relatively new to the industry. Cloud (2007 and 2009) introduced a multiple output backward auto regression (MOBAR) technique for a lab scale rotor. The technique works well for the free decay vibration with multiple modes in the time domain. Pattinato, et al (2010) applied the MOBAR technique to a multiple stage industry centrifugal compressor. The paper focused on MOBAR methods, without comparison between MOBAR and SDOF methods.

Takahashi, et al (2011) applied the MDOF method for an industry compressor rotor in the frequency domain by feeding a unidirectional excitation into one end of the rotor so that both forward and backward modes coexist. The response was analyzed by multiple input multiple output (MIMO) FRF or single input single output (SISO) FRF methods to estimate δ. The results agreed well with prediction, no comparison between MIMO FRF and the regular SDOF FRF methods were provided.

In this paper, results from SDOF FRF and SDOF time domain methods for a multistage centrifugal compressor will be compared.

Cross Coupling Estimation

Per API 617, the cross coupling stiffness is calculated using equation (5), which is the modified Wachel formula , (Wachel and von Nimitz, 1980)

$$Qxy = \frac{BcC * HP * \rho_d}{Dc * Hc * N * \rho_s} \quad (5)$$

Where,

BcC is the constant of 3*63=189
HP is horsepower;
Dc is the impeller diameter (in);
Hc is the impeller tip width (in);
N is the rotating speed in RPM;
ρ_d / ρ_s is the density ratio.

A CFD study has been done to evaluate the seal cross coupling coefficients for one impeller of this compressor (Zhang, et al, 2012). The CFD results were used to estimate the front seal cross coupling coefficients. The Wachel formula and CFD results were compared against test data in this paper.

Exciter design

Compressor manufacturers have used magnetic devices as a means to introduce arbitrary excitations of rotating systems in turbo-machinery since quite some time. In late 2007, the gas compressor group of the authors' company started detailed design considerations to create a system for the current product line of multistage compressors.

The basic concept comprises of a shaft extension to be attached to the non-driving end of the compressor by means of an adapter as well as a magnetic bearing stator to the end cap cavity. All compressors can be driven from either shaft end; therefore all shafts have coupling features that can be easily adapted to accept the shaft extension.

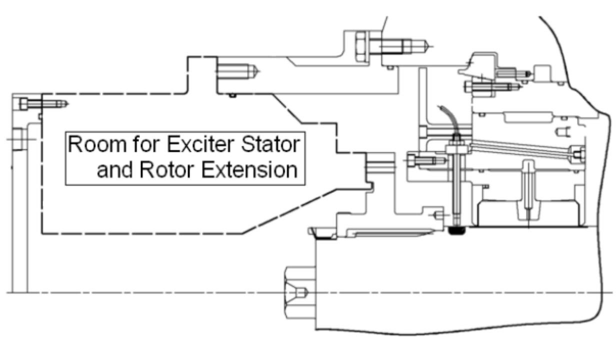

Figure 5. Compressor Non-driving End

To cover the range of compressors of interest, a force / frequency capability for the exciter system was specified that links respective rotor mass and max. operating speed of each compressor. This led to an initial requirement shown in Figure 6.

After some discussions about such a system with potential suppliers, a slightly reduced capability was agreed upon that promised sufficient capacity while utilizing pre-designed components. In order to keep the rotor dynamic influence of the added mass low, titanium was chosen for the main body of the rotor adapter. All mounting fits between the rotating adaptors and the respective shafts were carefully selected to allow ease of assembly while maintaining dynamic integrity as shown in Figure 7.

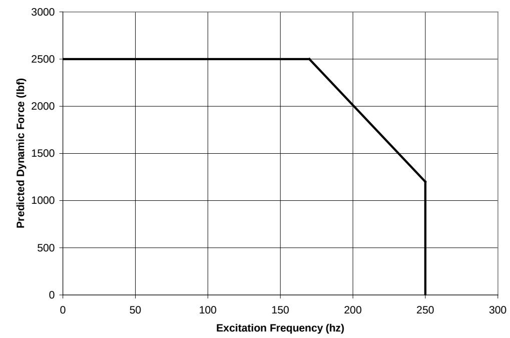

Figure 6. Requirement of Bearing Dynamic Capacity

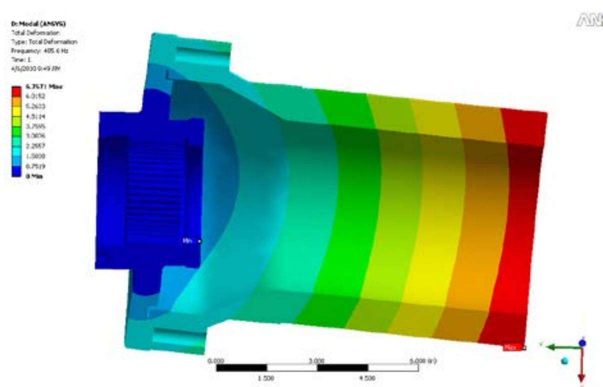

Figure 7: Modal Analysis of the 1st Bending Mode

In order to manage development risks and to accelerate the commissioning phase, a static support fixture (Figure 8) was designed that allowed pre-commissioning and basic training of the magnetic exciter system at the manufacturer's facility, well ahead of the actual application in the large test facility of the authors' company. This test stand also boasts a load cell to create a calibration capability (force demand signal as function of frequency vs. observed load).

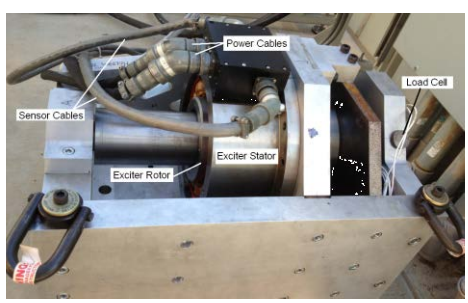

Figure 8. Exciter Calibration Rig

The magnetic bearing cabinet (power supply and controller for the magnetic exciter) is equipped with analog in- and outputs via BNC cables as well as a digital communication interface (MODBUS). Due to the exposure of the equipment (outside test facility), all cabling, connectors and intermediate junction boxes were carefully chosen to ensure reliable operation.

Rotor dynamic effect of the added Exciter

The exciter rotor plus mounting adapter will be attached to the non-driving end of the compressor. The mass of the rotor and adaptor is 67 lbs with polar moment of inertia of 745 lb-in^2 and transverse moment of inertia of 1459 lb-in^2. Calculations were done to see the effect of the added mass on a relatively large compressor rotor for a 5-Pad bearing with minimum clearance and 125°F oil. The added mass reduces δ by less than 3% as shown in Table 1. The impact on the natural frequency is very low.

Table 1: Added Mass effect on Rotor Stability

Min 125°F Oil, 5-Padbearing						
Exciter Rotor	Yes		No		Difference	
N (rpm)	Log Dec	cpm	Log Dec	cpm	Log Dec	cpm
7500	0.505	3918.5	0.508	3919.7	-0.59%	-0.03%
8000	0.468	3935.2	0.476	3935.2	-1.55%	0.00%
8500	0.431	3953.2	0.440	3953.8	-2.07%	-0.02%
9000	0.396	3970.4	0.406	3971.6	-2.40%	-0.03%
9500	0.365	3987.0	0.375	3988.8	-2.64%	-0.05%

After all design considerations were concluded, the system was ordered and manufactured. Figure 9 depicts stator and rotor for the magnetic exciter

Figure 9. Stator and Rotor of a MagneticExciter

The exciter stator is mounted on the compressor end cap and the exciter rotor is attached to the compressor rotor through an adaptor as shown in Figure 10. Currents to the stator coils are controlled to provide different forcing functions. Magnetic force is generated between the exciter stator (coils) and the rotor. The maximum static force the exciter can apply is 2000lbs (8.9KN) - powerful enough to excite any rotor currently in production at the author's company.

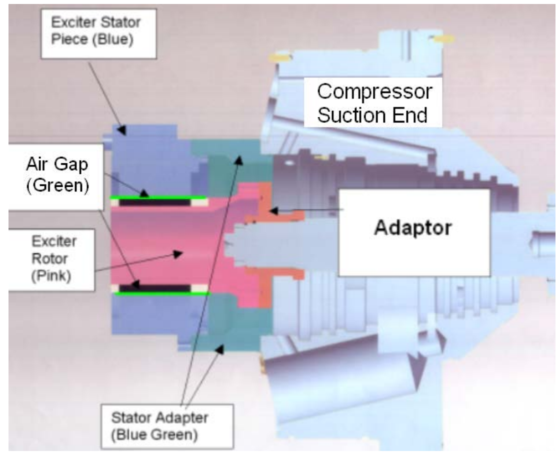

Figure 10. Magnetic Exciter on A Compressor

After commissioning of the magnetic exciter system, a multistage compressor was tested in the company's closed-loop test facility as shown in Figure 11 and Figure 12. The loop is rated at 3000psi (20.7Mpa). An 18,000-HP gas turbine drives the compressor through a gearbox.

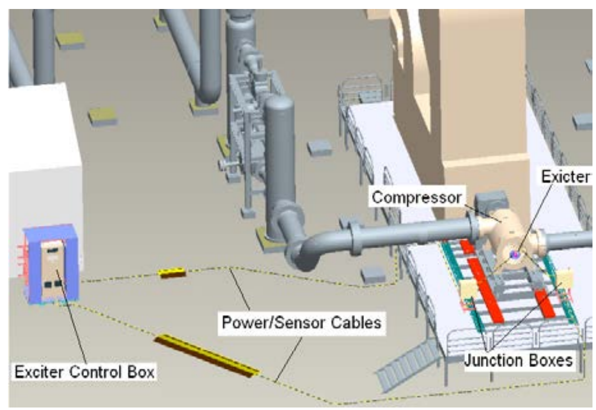

Figure 11. Test Facility and Exciter Test Setup

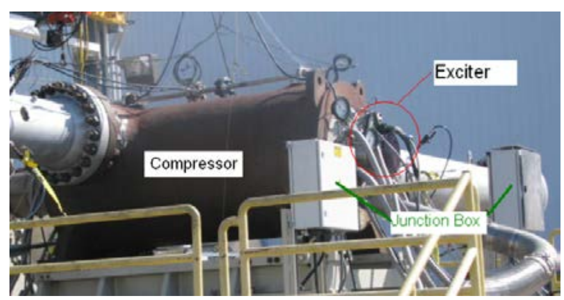

Figure 12. A Multistage Compressor with Magnetic Exciter on Test Stand

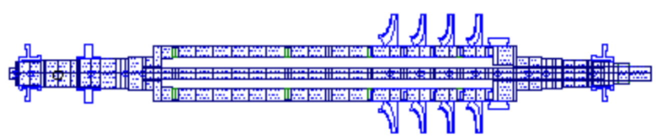

Figure 13. Rotor Model of The Tested Compressor

The compressor rotor has 4 impellers, as shown in Figure 13, the rest of the impeller span is filled with spacers. Other parameters of this test rotor are shown in Table 2.

Table 2: Tested Rotor Parameters

Bearing Span	87.46 in	2.22 m
Hub Diameter	9.13 in	0.23 m
Rotor Weight	1351 lb	613 kg
Max Speed	9500 rpm	

The compressor was running at different speeds and pressure along the 17,000HP (12.7MW) line as shown in Figure 14.

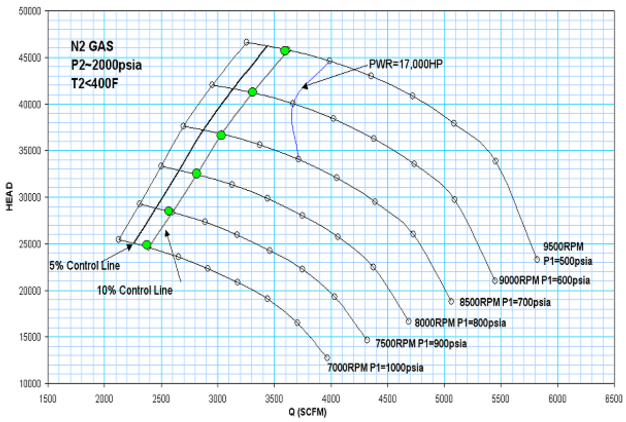

Figure 14. Test Compressor Aero Map

One of the main purposes of this test was the evaluation of alternative bearing designs. Three tilting pad journal bearings, one 5-pad and two 4-pad design, were tested as shown in Table 3. The only difference between the two 4-pad bearings is the pad length. The differences between 5-pad and 4-pad are pad numbers and load orientation. All three bearings share the same parameters such as offset, preload, bearing diameter, oil supply flow rate and oil inlet temperature.

Table 3: Tested Bearing Parameters

Bearing	5-Pad	4-Pad Normal	4-Pad Short
Number of Pads	5	4	
Load Position	On Pad	Between Pads	
L/D	0.76		0.50
Offset	0.5		
Nominal Preload	0.292		
Nominal Radial Clearance	0.0379		
Bearing Diameter	4.5in (114.3mm)		
Lubricant	ISO 32 Grade Turbine Oil		
Oil Inlet Temperature	125°F(51.7°C) to 145°F(63.8°C)		

TEST RESULTS AND BEARING COMPARISON

Sensitivity Tests

It was found that sensitivity tests are very important. For FRF sweeping tests, several sweeps were performed around the first critical frequency with different force levels and frequency resolutions. If the vibration level at the excitation frequency for this compressor is higher than 0.5 mil peak-to-peak and the sweeping frequency interval is less than 1 Hz, repeatable values of δ were obtained (the variation is within 1.5%).

Before excitation via transient tests, a sweeping test must be undertaken to identify the 1st critical natural frequency. It is very important to excite the rotor at the frequency of the 1st critical mode. If the excitation frequency is too far away from the critical frequency, the critical frequency likely will be either not excited or excited in a very low level as shown in Figure 15. According to our data, it is important to keep the excitation frequency within 10% of the 1st critical frequency to achieve consistent results.

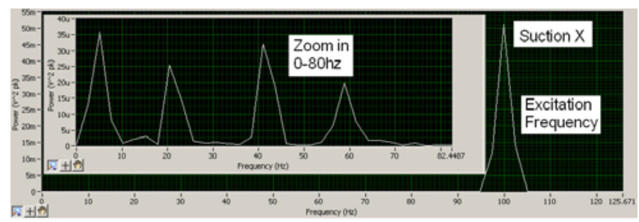

Figure 15. Sensitivity Study on How Transient Excitation Affects Log Dec Measurement

Excitation and Mode

Four types of excitations were evaluated during FRF sweeping tests and transient tests:

- Forward circular
- Backward circular and
- Uni directional excitation for each exciter axis

For forward circular excitation at the 1st critical frequency, the phase angle stays at 90° with the discharge end X component leading the discharge end Y component during steady and transient state (top part of Figure 16). This confirms that the forward circular excitation excites the forward mode.

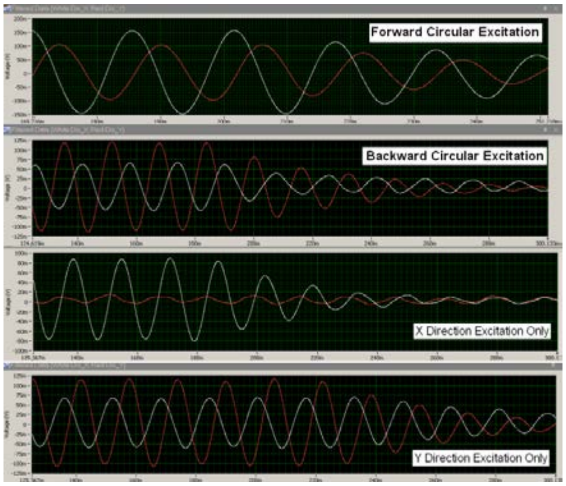

Figure 16. Excitation Methods and Excited Modes

For backward circular excitation, the X direction vibration leads the Y direction excitation by 270°, indicating that the backward mode is dominant over the steady excitation period. When the backward excitation is taken off, the forward mode starts to show and becomes dominant eventually. The backward sweeping excitation method is suggested to evaluate the backward mode δ. When excited in one direction, either the forward mode (Y direction excitation) or the backward mode can be excited (X direction excitation, bottom part of Figure 16).

Single Degree of Freedom System

Figure 17 shows the derived δ obtained from different sensors and different excitation methods for the compressor with 4-Pad L/D=0.5 bearings. The δ values are very close (within 0.05), consistent for all the tests. This indicates that the compressor rotor can be treated as a SDOF system if the excitation tests are conducted carefully. In the remainder of this paper only the averaged δ values are reported.

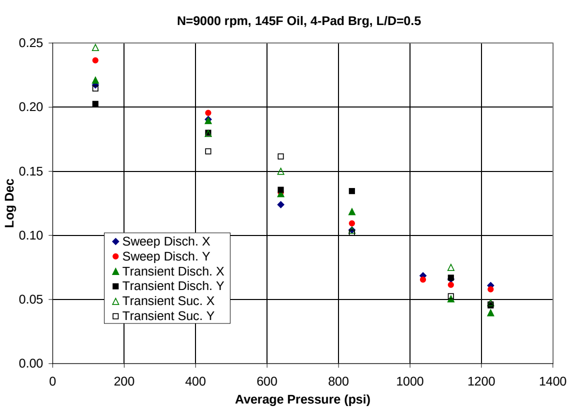

Figure 17. δ Comparison

Bearing Comparison

As shown in Figure 18, the rotor with 5-Pad bearings was much more stable than the one on 4-pad bearings. The long 4-Pad bearing (L/D=0.76) was slightly better than the short 4-Pad bearing.

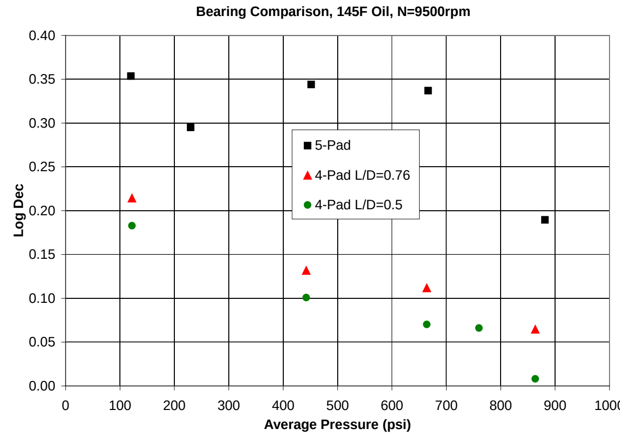

Figure 18. Bearing Comparison at 9500 rpm with 145 deg°F Oil

The δ of the rotor with different length 4-Pad bearings reaches the 0.1 threshold at an average pressure of 430 psi (L/D=0.5) and 660 psi (L/D=0.76). At this level of stability, the 1st critical frequency signal starts to appear in the vibration spectrum analysis as shown in Figure 19. This correlates well with API's mandate of Level II screening for δ approaching 0.1.

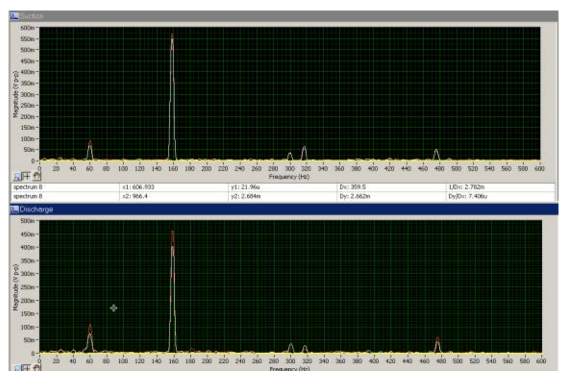

Figure 19. Sub-synchronous Signal, 4-Pad Bearing, L/D=0.76

Comparison between Analytical and Theoretical Results

In all of the following calculations, THPAD from ROMAC is used to calculate the tilting pad journal bearing coefficients. Figure 20 shows the labyrinth seal cross coupling effect on rotor stability with 5-Pad bearing at 9000 rpm. It can be clearly seen that Wachel's formula, equation (5) (API) predicts a less stable rotor than what was observed. This is consistent for all three speeds.

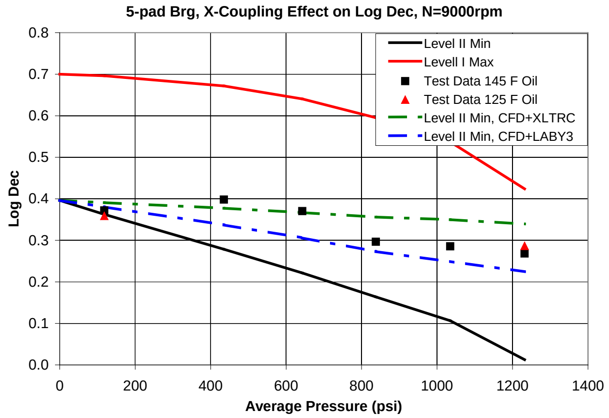

Figure 20. Theoretical vs Test Results, Log Dec, 5-Pad Brg, N=9000rpm

CFD simulations were done (Zhang, et al, 2012) to calculate the forces generated in the impeller eye seals and front cavity. The calculated forces are non-dimensionalized as:

$$\left(\frac{F}{e}\right)_{Non-D} = \frac{(F/e)}{\left(\frac{(P_0 + P_2)}{2A_P C_C}\right)} \quad (6)$$

where,

P_0 is the inlet static pressure

P_2 is impeller exit static pressure

A_P is impeller projected area in x-z or y-z plane

C_C is the seal clearance

The non-dimensional forces were plotted against the rotor whirl ratio and the dynamic coefficients are calculated based on the best-fit curves. One set of coefficients for the third stage of the rotor configuration shown on Figure 13 was listed in Table 4 (operating condition 9500 rpm, about 4000 scfm of Figure 14), comparing the relative contributions of eye seal and front shroud-stator cavity. It shows that the cavity contributes large dynamic forces. The cavity creates more direct damping and less direct stiffness.

The cross-coupling stiffness in the cavity is about one and half times of the stiffness in the shroud seal. The cavity also creates larger positive damping to stabilize the rotor. The results strongly indicate that the forces in the cavity cannot be ignored, more research should be conducted.

Table 4: Tested Bearing Parameters

Non-Dimensional	M [s^2]	C [s]	K
Cavity Portion + Seal Portion			
Direct	-5.56E-10	5.64E-06	1.07E-03
Cross-Coupling	-2.62E-09	3.59E-07	3.71E-03
Seal Portion			
Direct	-1.13E-09	1.87E-06	7.98E-04
Cross-Coupling	1.36E-10	-1.09E-06	1.49E-03
Cavity Portion			
Direct	5.73E-10	3.78E-06	2.72E-04
Cross-Coupling	-2.75E-09	1.45E-06	2.22E-03
Cavity/Seal Ratio			
Direct	-0.51	2.02	0.34
Cross-Coupling	-20.19	-1.33	1.49

Additional operating conditions were calculated for a matrix using CFD (significant CPU effort), dynamic coefficients were then interpolated for the shroud seals and cavities. Hub seal and the balance piston coefficients were created using LABY3 and XLTRC for comparison (see Figure 20 and Figure 21). Using coefficients from CFD and LABY3 predicts slightly lower δ than using coefficients from CFD and XLTRC. The slopes of both curves match data better than the API level I approach. As shown in Figure 21, the 1st critical frequency falls within the envelope of predictions.

Similar calculations were done for the 4-Pad long bearing (L/D=0.76). As seen in Figure 22, most of the values fall within the envelope formed by two CFD curves. The slopes of δ as a function of excitation frequency agree well with CFD curves.

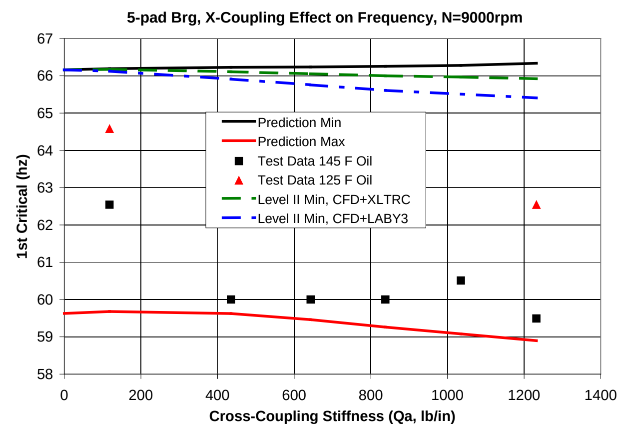

Figure 21. Theoretical vs Test Results, Frequency, 5-Pad Brg, N=9000rpm

All of the above indicates that if the bearing coefficients can be accurately predicted, the cross coupling effect can be predicted very well using CFD methods.

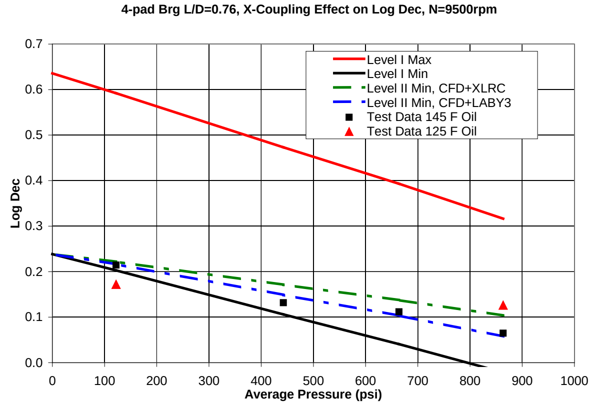

Figure 22. Theoretical vs Test Results, Log Dec, 4-Pad Brg L/D=0.76, N=9000rpm

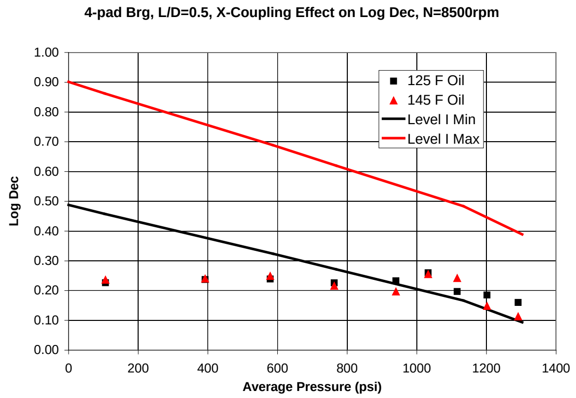

Figure 23. Theoretical vs Test Results, Log Dec, 4-Pad Brg L/D=0.5, N=9000rpm

For the short bearing, the cross coupling effect was not compared with CFD predictions since the bearing coefficient prediction is often too high. Only a Level I analysis was done. From Figure 23, we can see clearly that the slope predicted by Wachel's method is much larger than the test data in terms of δ value. This again confirmed that Wachel's formula tends to under-predict δ.

API Level I Screening Criteria

The stable points of rotor with 5-Pad bearings are shown in Figure 23. δ values for each point are listed in the legend. Even for the points in the Level II region, the compressor is still stable at the three different speeds tested.

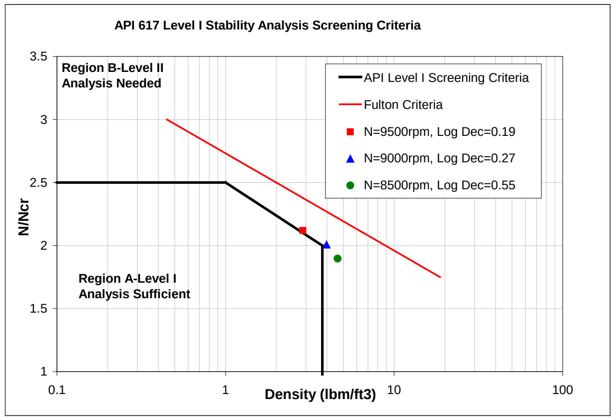

Figure 24. API Screening Criteria

CONCLUSIONS

Sensitivity tests (force, frequency interval, etc) must be conducted prior to data collection. To ensure consistent results, the rotor needs to be excited on its critical frequency when using transient method.

Forward circular excitation mainly excites the forward mode while backward circular excitation mainly excites the backward mode. The rotor can be treated as SDOF system. Transient and FRF sweeping methods give similar results in δ when the system is moderately stable (Log Dec <0.6). For a robust system (Log Dec >0.6), the transient method is preferred for the evaluation of system stability.

For the rotor studied in this paper, the 5-Pad tilting bearing outperformed 4-Pad bearings given the same clearance, preload and offset. 5-Pad bearings are chosen for this compressor.

For some bearings like the 5-Pad bearing, commercially available codes provide good predictions of coefficients but did not perform well for the 4-Pad short bearing. Testing is still very important for validation of bearing designs.

The API Level I criterion for the calculation of cross coupling effects tends to under-predict δ. CFD results lead to closer agreement with test data. More studies using CFD are needed for seal cross coupling effects.

NOMENCLATURE

AF	=Amplification Factor
D	=Diameter
HP	=Horsepower
L	=Length
Qxy	=Cross coupling stiffness
α	=Growth Factor
δ	=Logarithmic decrement (Log Dec)
ρ	=Density, 1/υ
σ	=System damping exponent
ω	=Excitation or Critical Speed
ξ	=Damping Ratio

REFERENCES

API, 2002, "Axial and Centrifugal Compressors and Expander-compressors for Petroleum, Chemical and Gas Industry Services", STD 617 7th Edition, American Petroleum Institute.

Atkins, K.E., Perez, R.X., 1990, "Assessing Rotor Stability Using Practical Test Prodedures", Proceedings of the 21st Turbomachinery Symposium, Turbomachinery Laboratory, Department of Mechanical Engineering, Texas A&M University, College Station, TX.

Baumann, U, 1999, "Rotordynamic Stability Tests on High-Pressure Radial Compressors", Proceedings of the 28th Turbomachinery Symposium, Turbomachinery Laboratory, Department of Mechanical Engineering, Texas A&M University, College Station, TX.

Bidaut, Y., Baumann, U., Al-Harthy, S. M. H., 2009, "Rotordynamic Stability of a 9500 PSI Reinjection Centrifugal Compressor Equipped with Hole Pattern Seal–Measurement Versus Prediction Taking into Account the Operational Boundary Conditions", Proceedings of the 38th Turbomachinery Symposium, Turbomachinery Laboratory, Department of Mechanical Engineering, Texas A&M University, College Station, TX.

Cloud, H.C., 2007, "Stability of Rotors Supported by Tilting Pad Journal Bearings", Ph.D. Dissertation, University of Virginia.

Cloud, H.C., Maslen, E.H., Barrett, L.E., 2009,"Damping Ratio Estimation Techniques for Rotordynamic Stability Measurements", J. of Engineering for Gas Turbines and Power.

Gupta, M.K., Thomas, S.A., Childs, D.W., 2008, "New Steps to Improve Rotordynamic Stability Predictions of Centrifugal Compressors", J. of Engineering for Gas Turbines and Power.

Moore, J. J., Walker, S. T., and Kuzdzal, M. J., 2002, "Rotordynamic Stability Measurement During Full-Load, Full-Pressure Testing of a 6000 Psi Re-Injection Centrifugal Compressor", Proceedings of the 31st Turbomachinery Symposium, Turbomachinery Laboratory, Department of Mechanical Engineering, Texas A&M University, College Station, TX.

Moore, J. J., and Soulas, T.A., 2003, "Damper Seal Comparison in a High-Pressure Re-Injection Centrifugal Compressor during Full-Load, Full-Pressure Factory Testing Using Direct Rotordynamic Stability Measurement," Proceedings of DETC'03, ASME 2003 Design Engineering Technical Conferences and Computers and Information in Engineering Conferences, Chicago, IL.

Pettinato, B.C., Cloud, C. H., Campos, R. S., 2010, "Shop Acceptance Testing of Compressor Rotordynamic Stability and Theoretical Correlation", Proceedings of the 39th Turbomachinery Symposium, Turbomachinery Laboratory, Department of Mechanical Engineering, Texas A&M University, College Station, TX.

Soulas, T.A., Kuzdzal, M.J., 2009, "Rotordynamic Testing and Evaluation of A Large Centrifugal Compressor Using A Magnetic Bearing Exciter", GT2009-60320, Proceedings of ASME Turbo Expo 2009: Power of Land, Sea and Air, Orlando, FL.

Sorokes, J.M., Soulas, T.A., Koch, J.M., Gillarranz R, J.L., 2009, "Full-Scale Aerodynamic and Rotordynamic Testing for Large Centrifugal Compressors", Proceedings of the 38th Turbomachinery Symposium, Turbomachinery Laboratory, Department of Mechanical Engineering, Texas A&M University, College Station, TX.

Takahashi, N., Magara, Y., Narita, M., and Miura, H., 2011, "Rotordynamic Evaluation of Centrifugal Compressor Using Electromagnetic Exciter", GT2011-45829, Proceedings of ASME Turbo Expo 2011: Power of Land, Sea and Air, Vancouver, British Columbia, Canada.

Wachel, J.C. and von Nimitz, W.W., 1980, "Assuring the Reliability of Offshore Gas Compression Systems," European Offshore Petroleum Conference & Exhibition, London, England.

Zhang, D, Lee, C, and Cave, M.J., 2012, "A CFD Study on The Dynamic Coefficients of Labyrinth Seals", GT2009-60320, Proceedings of ASME Turbo Expo 2012: Power of Land, Sea and Air, Copenhagen, Denmark.

ACKNOWLEDGMENTS

The authors wish to thank Solar Turbines Incorporated for the permission to publish this paper. A huge team effort of engineers, technicians and management supported this project over a long time, they are to be commended for their patience and dedication. In particular, we would like to thank Roman Braunstein, Jack Goode and our former colleague, Sam Hoffman for their thorough work that helped to create this useful tool.